doi:10.1246/cl.2011.292

Published on the web February 16, 2011

Photoinduced Triplet States of Photoconductive TTF Derivatives Including a Fluorescent Group

Ko Furukawa,*[1,2] Yasuo Sugishima,[3] Hideki Fujiwara,[3] and Toshikazu Nakamura[1,2]
[1]*Institute for Molecular Science, 38 Nishigo-naka, Myodaiji, Okazaki, Aichi 444-8585*
[2]*The Graduate University for Advanced Studies, 38 Nishigo-naka, Myodaiji, Okazaki, Aichi 444-8585*
[3]*Graduate School of Science, Osaka Prefecture University, 1-1 Gakuen-cho, Naka-ku, Sakai, Osaka 599-8531*

(Received December 21, 2010; CL-101080; E-mail: kou-f@ims.ac.jp)

The spin dynamics of photoconductive tetrathiafulvalene (TTF) derivatives containing 2,5-diphenyl-1,3,4-oxadiazole (PPD) was examined using time-resolved electron spin resonance (TR-ESR) spectroscopy. TR-ESR signals of a frozen solution sample under visible excitation were attributed to the excited triplet state $\mathbf{T_1}$, which was populated via intersystem crossing from the excited singlet state $\mathbf{S_1}$ as confirmed by TR-ESR spectral simulations. From DFT calculations, the spin-density distribution of the $\mathbf{T_1}$ state was found to be concentrated around the linker between the TTF and PPD molecules.

Photofunctional materials have attracted considerable attention not only from a purely fundamental perspective but also for their practical application. Such materials are of great interest in devices such as solar cells and field-effect transistors (FETs), and as such photofunctional molecules have been extensively investigated.[1] The biggest issue for many applications is the low photoinduced electron-transfer efficiency of these materials, i.e., the photoelectric conversion efficiency in regards to solar cells or the photocurrent efficiency in photoconductive materials. For the continued development of high-efficiency photofunctional materials, it is vital to clarify the mechanism of their photoinduced electron transfer. An important factor in such mechanisms is the existence of a "charge-separated (**CS**) state." Popular models for investigating photoinduced intramolecular charge transfer and the resulting charge-separated state[2] are donor–acceptor type dyads, such as those based on tetrathiafulvalene (TTF) frameworks. Recently, Fujiwara et al. have reported on new TTF derivatives that include a fluorescent group such as 2,5-diphenyl-1,3,4-oxadiazole (PPD) (Figure 1). These derivatives are well known as electron-transport materials in electroluminescence devices and thus are good candidates for photoelectric conversion materials.[3] Based on UV–vis absorption spectra, emission spectra, and photocurrent action spectra, it was found that the TTF derivative **1** exhibited photoconductivity.[3a] However, the mechanism by which photoconductivity is mediated has not been revealed yet. In the present paper, two TTF derivatives **1** and **2** are examined using pulsed time-resolved ESR (TR-ESR) spectroscopy from the viewpoint of spin dynamics. The relationship between the spin dynamics and the linker between the two groups is investigated.

ESR measurements are an extremely sensitive probe for examining the local environment surrounding the electron spin. Actually, conventional ESR spectroscopy is used to estimate the carrier density in molecular devices such as FETs.[4] Pulsed TR-ESR spectroscopy is an advanced ESR technique which probes the electron dynamics after a laser flash, making it possible to examine the excited states.[5] Photocurrent efficiency depends on both lifetime and efficiency of the **CS** state. By using pulsed TR-ESR, important information on the mechanism of electron transfer can be obtained microscopically.[6] In particular, the spin population, the lifetime of the spin, and the zero-field splitting parameter, D, in the transient state could be determined directly. Ultimately, we would like to reveal the mechanism of photoinduced electron transfer in terms of the spin dynamics. In the present study, we use pulsed TR-ESR spectroscopy to examine the spin dynamics of toluene solution samples of TTF derivatives including a PPD group. The results show that both materials attain an excited triplet ($\mathbf{T_1}$) state, induced by intersystem crossing from the excited singlet state, and that the **CS** state does not arise for the isolated system.

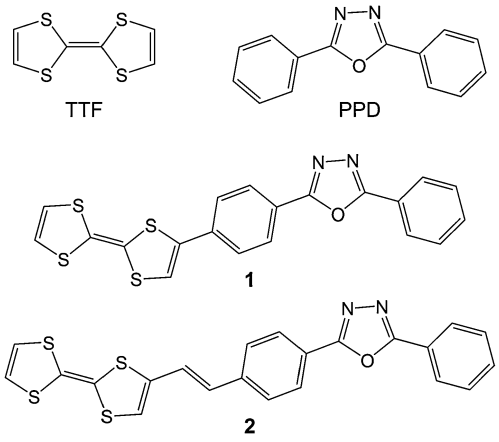

Figure 1. Molecular structures of TTF derivatives **1** and **2**.

The absorption spectra for TTF, PPD, **1**, and **2** in CH_2Cl_2 solution at room temperature are shown in SI.[7] Two dominant absorption bands, i.e., the excitation band of the individual TTF and PPD groups in the UV region (ca. 300 nm) and a band corresponding to charge transfer (CT) from the TTF to PPD groups in the visible region (ca. 500 nm), were observed for both samples. These results are consistent with those described in a previous report.[3] Figure 2a shows the two-dimensional pulsed TR-ESR spectrum for **2** at 532-nm excitation. The horizontal and vertical axes denote the magnetic field and the time after the laser flash, respectively, while the normal axis indicates the ESR signal intensity. Before the laser flash, i.e., $t < 0$, no ESR signal was observed over the entire magnetic field range. After the laser flash, the ESR signal intensity suddenly increases up to $t = 0.5\,\mu s$ before decaying after this time. Figures 2b and 2c show the slice spectra along the magnetic field axis at $t = 0.5\,\mu s$ for **1** and **2**. In addition to the signals at around $g \approx 2.00$, the ESR signal corresponding to the $|\Delta m_s| = 2$ transition was also

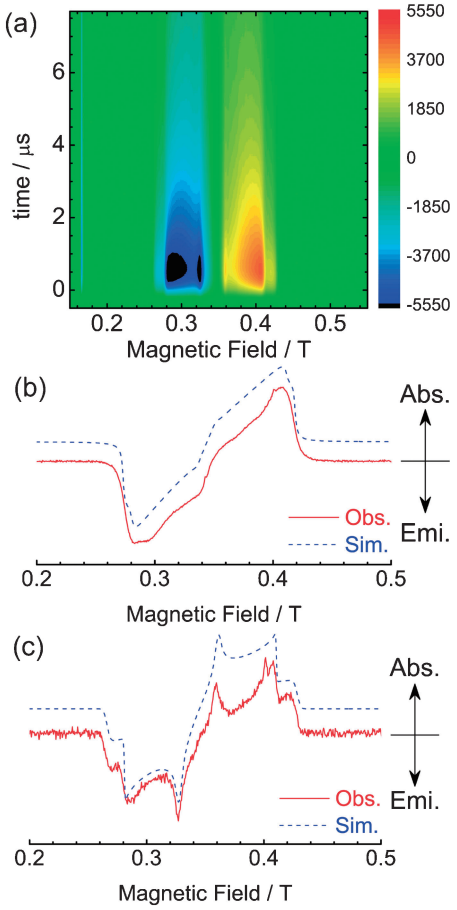

Figure 2. (a) 2D pulsed TR-ESR spectra for **2**. The normal axis represents the ESR signal intensity. The color scale denotes the signal intensity. Positive and negative values indicate the absorption and emission of microwaves, respectively. Slice spectra along the magnetic field axis at $t = 0.5\,\mu s$ and $T = 20\,K$ for (b) **1** and (c) **2**, respectively. The solid and dotted lines denote the observed and simulated spectra, respectively.

observed at 0.17 T for both samples. On the other hand, no ESR signals were observed for either of the only TTF and PPD molecules over the entire magnetic field range. These results indicate that materials **1** and **2** have a singlet ground state $\mathbf{S_0}$ and the observed ESR signals originate from the excited triplet state $\mathbf{T_1}$ of the TTF derivatives.

In order to obtain detailed information on the excited state, we performed a spectral simulation based on the triplet model.[8] The spin Hamiltonian of the triplet state can be expressed as follows:

$$H = \mu_B \mathbf{S} \cdot \mathbf{g} \cdot \boldsymbol{B_0} + \mathbf{S} \cdot \mathbf{D} \cdot \mathbf{S} \quad (1)$$

where the first and second terms denote the Zeeman and zero-field splitting (ZFS) terms, respectively. μ_B, $\mathbf{S}$, $\mathbf{g}$, $\mathbf{D}$, and $\boldsymbol{B_0}$ stand for the Bohr magneton, spin operator, **g**-tensor, ZFS tensor, and magnetic field, respectively. The principal values of the ZFS tensor are expressed as $(-D/3 + E,\ -D/3 - E,\ 2D/3)$. Figures 2b and 2c show the simulated spectra for **1** and **2** together with the measured spectra. The estimated spin-Hamiltonian parameters and the ratio of the population factor are

Table 1. Spin-Hamiltonian parameters estimated from spectral simulation

Sample	**1**	**2**
S	1	1
g-tensor	(2.003, 2.006, 2.006)	(2.008, 2.006, 2.006)
$\lvert D\rvert/\mathrm{cm}^{-1}$	0.068	0.076
$\lvert E\rvert/\mathrm{cm}^{-1}$	0.018	0.015
Linewidth/G	(40.0, 60.0, 25.0)	(10.0, 35.0, 45.0)
$P_x/P_z{:}P_y/P_z$ $(D < 0)$	0.14:0.29	0.37:0.12

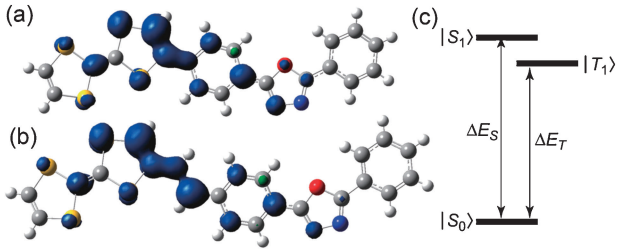

Figure 3. Calculated spin-density distribution for (a) **1** and (b) **2** based on the DFT. (c) Schematic energy diagram for TTF derivatives for **1** and **2**.

Table 2. Calculated energy gap (eV) for **1** and **2** based on the DFT

Sample	**1**	**2**
$\Delta E_{S_0-S_1}$	2.27	2.30
$\Delta E_{S_0-T_1}$	1.88	1.88
$\Delta E_{S_1-T_1}$	0.39	0.42

summarized in Table 1. The simulated spectra for **1** and **2** are in good agreement with the measured spectra. Notably, the measured spectra are reproduced by triplet species with $|D|$ values of 0.068 and 0.076 cm^{-1} for **1** and **2**, respectively. Under the point-dipole approximation, a $|D|$ value of ca. 0.07 cm^{-1} corresponds to a mean spin–spin distance of ca. 6.5 Å. In this case, the $|E/D|$ value, which describes the deviation from axiality of the spin–spin interaction, is larger for **1** than for **2**. In the case of the excited triplet state, it is difficult to determine the sign of the D value experimentally due to the extremely narrow energy gap. We will discuss these results later together with the spin-density distribution.

In order to examine the excited state, DFT calculations were performed for **1** and **2**. The calculated molecular orbital and energy diagrams for both samples are shown in SI.[7] The highest occupied molecular orbital (HOMO) is concentrated on the TTF group while the lowest unoccupied molecular orbital (LUMO) is distributed from the tail of TTF to the edge of PPD via the linker. Excitation in the visible corresponds to HOMO–LUMO transition while excitation in the UV corresponds to transitions of the TTF and PPD groups. According to these calculations, the TTF derivative has a singlet ground state $\mathbf{S_0}$, a first excited state $\mathbf{T_1}$, and a second excited state $\mathbf{S_1}$ as Figure 3c. The energy gaps between these states are summarized in Table 2. The $\mathbf{S_1}$ and $\mathbf{T_1}$ states are 2.3 and 1.9 eV higher in energy, respectively, than the $\mathbf{S_0}$ state for both samples. The first excited state could be

regarded as the $\mathbf{T_1}$ state. However, because of the zero transition probability for $\mathbf{S_0}$–$\mathbf{T_1}$, the photoinduced excited state is the $\mathbf{S_1}$ state, which is expected to populate the $\mathbf{T_1}$ state by intersystem crossing. In order to obtain more detailed information on the $\mathbf{T_1}$ state, the spin distribution of the $\mathbf{T_1}$ state was estimated by an unrestricted DFT calculation using UB3LYP. Figures 3a and 3b show the spin-density distribution for **1** and **2**. In both cases, the spin density is concentrated on the π orbital extending from the tail of the TTF group to the edge of the PPD group via the linker. A slight difference in the $|D|$ values between **1** and **2** reflects the slight difference in spin density on the alkene linker. Because of the prolate spin-density distribution on the π orbital, a negative D value might be expected.[5a] Thus, due to the long alkene linker in molecule **2**, the LUMO orbital of **2** has higher axiality, i.e., a smaller $|E/D|$ value, than that of **1**.

In this section, we discuss the spin dynamics of the $\mathbf{T_1}$ state based on signal intensity. The observed pulsed TR-ESR spectral patterns for both samples were expressed as an EEE/AAA pattern, where E and A denote the emission and absorption of microwaves, respectively. Assuming $D < 0$, the estimated population factors are summarized in Table 1. In both samples, the population factor P_z is the dominant factor, indicating experimental evidence for intersystem crossing from $\mathbf{S_1}$ to the $m_s = 0$ sublevel of the $\mathbf{T_1}$ state, as the direct $\mathbf{S_0}$–$\mathbf{T_1}$ transition is optically forbidden. Therefore, the signal decay can be expressed as an exponential function of the lifetime of the excited triplet state. The lifetime for **1** (ca. 40.8 µs) is close to that for **2** (ca. 35.7 µs) at 20 K.[7] The recombination rate for **2** is higher than that for **1**. This result coincides with the larger D value for **2**, i.e., the smaller mean spin–spin distance for **2**.

We also measured the pulsed TR-ESR spectrum at 355-nm excitation (Figure 4). The spectral patterns are similar for both excitations but the signal intensities differ considerably; the signal intensity at 355-nm excitation is five times smaller than that at 532 nm. This implies that the observed spectra originate in the excitation at the tail of the visible-light band. The **CS** state necessary for photoconductivity could not be observed in the isolated systems, which could be for the following two reasons. The first is the possibility of fast spin dynamics beyond the limits of the machine. The second possibility is that the **CS** state was not induced by photoexcitation of a single molecule but from the condensed matter state. Since the photoconductivity was observed at room temperature using a cw-light source,[3] the relaxation time of the **CS** state might be not so short. Therefore, the photoconductivity in these materials could be regarded as the electronic properties peculiar to the condensed state.

The spin dynamics of photoconductive TTF derivatives **1** and **2** was examined using pulsed TR-ESR spectroscopy. In both samples, the $\mathbf{T_1}$ state was confirmed as the first excited state, populated via intersystem crossing from $\mathbf{S_1}$. Also, high spin density is observed at the link between the TTF and PPD groups. In the frozen solution samples, a **CS** state could not be detected for either visible or UV excitation. For UV excitation, the population of the $\mathbf{T_1}$ state decreased. On the other hand, the intramolecular charge transfer might be assisted by a condensation effect arising in the solid. To clarify this, we have obtained preliminary pulsed TR-ESR spectra with a small D value for a powder sample under UV excitation. Detailed investigations on this sample are currently underway.

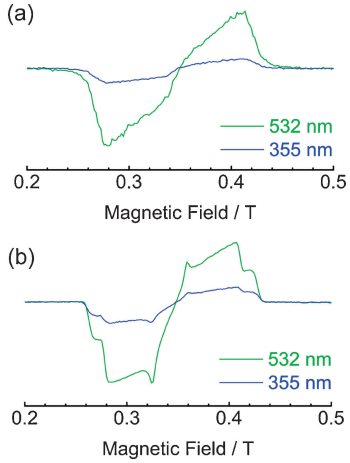

Figure 4. Wavelength dependence of pulsed TR-ESR spectra at 1 µs for (a) **1** and (b) **2**. Green and blue lines denote the pulsed TR-ESR spectra at 532 and 355 nm excitation, respectively.

This work was supported by a Grant-in-Aid for Scientific Research in Innovative Areas, "New Frontier of Materials Science Opened by Molecular Degrees of Freedom" (Nos. 21110523 and 20110006) and a Grant-in-Aid for Young Scientists (A) (No. 21685021). One of the authors (T. N.) was supported by a Grant-in-Aid for Scientific Research (B) (No. 20340095) from the Ministry of Education, Culture, Sports, Science and Technology, Japan.

References and Notes

1 Example for: a) U. Bach, D. Lupo, P. Comte, J. E. Moser, F. Weissörtel, J. Salbeck, H. Spreitzer, M. Grätzel, *Nature* **1998**, *395*, 583. b) K. P. Pernstich, S. Haas, D. Oberhoff, C. Goldmann, D. J. Gundlach, B. Batlogg, A. N. Rashid, G. Schitter, *J. Appl. Phys.* **2004**, *96*, 6431.

2 a) J. R. Durrant, S. A. Haque, E. Palomares, *Chem. Commun.* **2006**, 3279. b) L. Valentini, D. Bagnis, A. Marrocchi, M. Seri, A. Taticchi, J. M. Kenny, *Chem. Mater.* **2008**, *20*, 32. c) M. R. Bryce, *Adv. Mater.* **1999**, *11*, 11. d) H. Nishikawa, S. Kojima, T. Kodama, I. Ikemoto, S. Suzuki, K. Kikuchi, M. Fujitsuka, H. Luo, Y. Araki, O. Ito, *J. Phys. Chem. A* **2004**, *108*, 1881.

3 a) H. Fujiwara, Y. Sugishima, K. Tsujimoto, *Tetrahedron Lett.* **2008**, *49*, 7200. b) H. Fujiwara, K. Tsujimoto, Y. Sugishima, S. Takemoto, H. Matsuzaka, *Physica B* **2010**, *405*, S12.

4 a) A. J. Maliakal, J. Y.-C. Chen, W.-Y. So, S. Jockusch, B. Kim, M. F. Ottaviani, A. Modelli, N. J. Turro, C. Nuckolls, A. P. Ramirez, *Chem. Mater.* **2009**, *21*, 5519. b) K. Marumoto, M. Kato, H. Kondo, S. Kuroda, N. C. Greenham, R. H. Friend, Y. Shimoi, S. Abe, *Phys. Rev. B* **2009**, *79*, 245204.

5 a) P. J. Angiolillo, V. S. Y. Lin, J. M. Vanderkooi, M. J. Therien, *J. Am. Chem. Soc.* **1995**, *117*, 12514. b) P. J. Angiolillo, H. T. Uyeda, T. V. Duncan, M. J. Therien, *J. Phys. Chem. B* **2004**, *108*, 11893.

6 a) K. Akiyama, S. Hashimoto, S. Tojo, T. Ikoma, S. Tero-Kubota, T. Majima, *Angew. Chem., Int. Ed.* **2005**, *44*, 3591. b) S. Moribe, T. Ikoma, K. Akiyama, S. Tero-Kubota, *Chem. Phys. Lett.* **2008**, *457*, 66.

7 See the Supporting Information. Experimental details, aborption spectra, MO calculation, and ESR signal decay (PDF). Supporting Information is available electronically on the CSJ-Journal Web site, http://www.csj.jp/journals/chem-lett/index.html.

8 D. H. Harryvan, W. H. Lubberhuizen, E. von Faassen, Y. K. Levine, G. Kothe, *Chem. Phys. Lett.* **1996**, *257*, 190.

